shift at site A and B below T_c in Figure 4.

Figure 5 shows a plot of the mole fraction of site B from Cu NQR intensity versus strontium doping. Of course the plot for site A is just the inverse since we defined the mole fraction of A as 1-B. The dashed line represents the calculated probability of 2-Sr in the second coordination sphere of copper, $P_2(x)$, from Table I. The mole fraction of site B calculated from the $P_2(x)$ is significantly less than observed. However, the probability distributions were calculated assuming random distribution of strontium atoms over all lanthanum sites. A model that includes attractive interactions, which could reflect a tendency of strontium atoms to cluster together, might achieve better agreement. The solid line is the value of strontium doping x, or the mole fraction of copper formally oxidized as a result of that doping. Interestingly, the observed mole fraction of site B correlates well with strontium substitution. We cannot distinguish between either model based solely on measured occupancies of the two sites.

Summary

We have demonstrated that the concentration of a second type of copper in the $La_{2-x}Sr_xCuO_{4-\delta}$ superconductor increases with increasing doping level. The magnetic shifts of both types of copper appear to be temperature independent in the normal state but have a steep drop below T_c. It is concluded from the similarity of their shift behavior (they have the same T_c) that both copper sites are located in the superconducting ($CuO_{4/2}$) plane. The existence of two microscopically distinct copper sites in this superconducting compound is unexpected considering the crystallographic structure.

Acknowledgment. This work was supported by the NSF-MRL program through the Northwestern Materials Research Center (Grant DMR-8821571). The Quantum Designs Magnetic Susceptometer was purchased by the NSF-STC program for superconductivity (Grant DMR-8809854).

Chemical Vapor Deposition of Platinum: New Precursors and Their Properties

Neil H. Dryden, Ravi Kumar, Eric Ou, Mehdi Rashidi, Sujit Roy, Peter R. Norton, and Richard J. Puddephatt*

Department of Chemistry, University of Western Ontario, London, Ontario, Canada N6A 5B7

John D. Scott

3M Canada Inc., C.P. Box 5757, London, Ontario, Canada N6A 4T1

Received February 14, 1991. Revised Manuscript Received May 14, 1991

The complexes *cis*-[PtMeRL$_2$], where R = Me, CH_2=CH, CH_2=$CHCH_2$, *t*-BuC≡C and L = MeNC or L_2 = 1,5-cyclooctadiene, are shown to be useful precursors for the chemical vapor deposition (CVD) of platinum films under mild conditions. Carbon impurities in the films and the temperature of CVD were both greatly reduced when CVD was carried out in the presence of hydrogen, but CVD was retarded in the presence of free MeNC. The σ-allylplatinum or σ-vinylplatinum complexes gave CVD at the lowest temperature. Thermolysis of *cis*-[$PtMe_2(MeNC)_2$] gives methane as a gaseous product, and this is shown to be formed by combination of a methylplatinum group with a hydrogen atom from H_2, if present, or from the cell wall. The carbon impurities in the platinum films formed by CVD in the absence of hydrogen were shown to be derived at least partly from the methylplatinum groups.

Introduction

Organometallic chemical vapor deposition (OMCVD) of thin-film metallic conductors has emerged as a useful technique for the fabrication of microelectronic components.[1,2] Recent studies[1b,3] in the OMCVD of III–V semiconductor materials have established that an understanding at the molecular level of the various chemical processes involved during the decomposition of the precursor is mandatory in controlling the growth and properties of the deposited semiconductor film. However, mechanistic studies have been few,[1b,4] and challenges remain in the detailed analysis of the various decomposition pathways, including separation of gas-phase and surface reactions, and in the kinetic modeling of CVD. There is a clear need for a better understanding of the fundamental

(1) (a) Sherman, A. *Chemical Vapor Deposition for Microelectronics: Principles, Technology, and Applications*; Noyes Publications: Park Ridge, New Jersey, 1987. (b) Gross, M. E., Jasinki, J. M., Yates, J. T., Eds. Chemical Perspectives of Microelectronic Materials. *Mater. Res. Soc. Symp. Proc.* **1989**, *131*. (c) Williams, J. O. *Angew. Chem., Int. Ed. Engl. Adv. Mater.* **1989**, *28*, 1110.

(2) (a) Jasinski, J. M.; Meyerson, B. S.; Scott, B. A. *Annu. Rev. Phys. Chem.* **1987**, *38*, 109. (b) Cole-Hamilton, D. J., Williams, J. O., Eds. *Mechanisms of Reactions of Organometallic Compounds with Surfaces*; NATO ASI Series B, 1989; Vol. 198.

(3) (a) Lee, P. W.; Omstead, T. R.; McKenna, D. R.; Jenson, K. F. *J. Cryst. Growth*, **1987**, *85*, 165. (b) Tsuda, M.; Oikawa, S.; Morishita, M.; Mashita, M. *Jpn. J. Appl. Phys.* **1987**, *26*, 6564.

(4) (a) Konstantinov, L.; Nowak, R.; Hess, P. *Appl. Phys.* **1988**, *A47*, 171. (b) Wood, J. *Vacuum* **1988**, *38*, 683. (c) Bent, B. E.; Nuzzo, R. G.; Dubois, L. H. *J. Am. Chem. Soc.* **1989**, *111*, 1634. (d) Speare, K. E.; Drix, R. R. *Pure Appl. Chem.* **1990**, *62*, 89. (e) Girolami, G. S.; Jensen, J. A.; Pollina, D. M.; Williams, W. S.; Kaloyeros, A. E.; Allocca, C. M. *J. Am. Chem. Soc.* **1987**, *109*, 1579. (f) Feurer, R.; Larhrafi, M.; Morancho, R.; Calsou, R. *Thin Solid Films* **1988**, *167*, 195. (g) Gladfelter, W. L.; Boyd, D. C.; Jensen, K. F. *Chem. Mater.* **1989**, *1*, 339. (h) Girolami, G. S.; Jeffries, P. M. *Chem. Mater.* **1989**, *1*, 8. (i) Sauls, F. C.; Interrante, L. V.; Jiang, Z. P. *Inorg. Chem.* **1990**, *29*, 2989.

0897-4756/91/2803-0677$02.50/0

mechanistic basis of CVD, with the aim of being able to tailor organometallic precursors for CVD of selected materials under controlled conditions.

Recently, we have been interested in the chemical vapor deposition of thin films of gold, rhodium, and platinum, which have applicability in microelectronics and other industries. During the course of these investigations, we and others noted that the metal films are usually contaminated with carbon and sometimes other elements.[5] It was further observed that the carbon contamination could be drastically reduced if CVD was carried out in an atmosphere of hydrogen.[5b,c] To develop an understanding of the fundamental basis of CVD of platinum, it was necessary to establish a relationship between the quality of the platinum films produced by CVD on such variables as the nature of the organoplatinum precursor and the temperature and pressure used for the CVD, as well as the enhancement of CVD in the presence of carrier gases including hydrogen, by UV irradiation or by the presence of a preformed platinum film. It was also desirable to determine the source and nature of the impurities in the films, and this requires a study of the mechanism of pyrolysis of the organoplatinum precursors in the presence and in the absence of hydrogen. The results of some of these studies are reported in this paper.

Prior to the present study, several organoplatinum(II) and -(IV) complexes have been used as precursors for the OMCVD of platinum.[6,7] Examples include $[Pt(hfacac)_2]$ (hfacac = $CF_3COCHCOCF_3$), $[Pt(CO)_2Cl_2]$, $[Pt(PF_3)_4]$, and more recently $[(\eta^3\text{-}C_3H_5)_2Pt]$, $[(\eta^5\text{-}Cp)PtMe_3]$, and $[(\eta^5\text{-}MeCp)PtMe_3]$.[5-7] Since other groups are concentrating on these systems, we have studied the σ-bonded organoplatinum(II) compounds of the type $[PtMe_2L_2]$ and $[PtR(Me)L_2]$. These complexes are easily synthesized, the volatility and thermal and photochemical stability can be controlled by varying the nature of the organic group R (R = alkyl, vinyl, alkynyl, or allyl) or the neutral ligands L (L = phosphines, dienes, isocyanides), and their use as CVD precursors has not been studied previously. The synthesis and characterization of the new alkylplatinum complexes used as precursors in the present study are also reported.

Experimental Section

All the reactions involving organomagnesium and lithium reagents were carried out using standard Schlenk techniques. Diethyl ether was dried by refluxing over sodium under nitrogen and then distilled.

The CVD precursors were synthesized and then characterized by spectroscopic methods. ^1H and ^{13}C NMR spectra were recorded by using Varian XL-200 and XL-300 instruments, respectively, and IR spectra by using Bruker IFS 32/IBM-9000 and Mattson Cygnus-100 FTIR spectrometers. MS and GC-MS spectra were recorded by using a Varian MAT 311A instrument.

The CVD precursors were then decomposed in the absence and presence of hydrogen. Ex situ techniques (GC, GC-MS, TGA-FTIR, DSC) were used to characterize the gas-phase products of decomposition, and XPS and SIMS analyses and conductance measurements were carried out on the deposited films. For ex situ analysis, films were usually prepared in a vertical, Pyrex CVD reactor with dynamic pumping, and the films produced were then transferred to the appropriate analytical facility. XPS spectra were obtained by using a SSL SSX-100 small-spot XPS surface-analysis instrument with a monochromatized Mg Kα X-ray source (1253.6 eV). Binding energies reported were reproducible to within ±0.1 eV. All the spectra were computer fitted to 70% Gaussian line shapes after subtracting a background proportional to the integral of the photoelectron peaks (Shirley background) and using no constraint to the final fit. The SIMS depth profile study was conducted using a CAMECA IMS-3f secondary ion microscopy/mass analyzer with Cs^+ or $^{16}O^-$ as primary ion source. SEM micrographs of platinum films were taken by using an ISL DS-130 scanning electron microscope. The thickness of the platinum films was measured with a DEKTAK II profilometer and conductances were measured by using the four-point probe method. TGA analysis was carried out by using a Du Pont 951 thermogravimetric analyzer, and DSC analysis by using a Du Pont Instruments 912 DSC in conjunction with the 9900 computer/thermal analyzer. Gas chromatography was performed on a Varian 3400 instrument using a EGDM porous polymer support and a 2-m-long column.

Gas-phase FTIR was used as an in situ technique to probe the decomposition process itself as well as to characterize the complexes in the gas phase and to determine the vapor pressure. For gas-phase IR spectra, a cell with path length of 10 cm and total internal volume of 76 mL was constructed to fit in the cell compartment of the Mattson instrument. The performance of the cell toward "vacuum-hold" was found to be satisfactory over a pressure range of 2×10^{-3}–500 Torr and a temperature range of 293–623 K. Compounds were transported into the cell as solids or as solutions in benzene. The cell was subsequently evacuated to an internal pressure of 2×10^{-3} Torr at room temperature and then externally heated, using heating tapes, to vaporize the precursor and so allow the gas-phase IR spectrum to be recorded. All spectra are recorded following data collection for 320 scans at 4-cm^{-1} resolution by using the Mattson spectrometer. The in situ decomposition was monitored in the same way by heating to higher temperatures and then monitoring changes in the FTIR spectra as a function of time.

The complexes *trans*-$[Pt(Me)Cl(SMe_2)_2]$, $[Pt(Me)Cl(COD)]$, *cis*-$[PtMe_2(MeNC)_2]$, *cis*-$[PtMe_2(2,6\text{-}Me_2\text{-}C_6H_3NC)_2]$, and $[PtMe_2(COD)]$ were prepared by literature methods.[8]

***cis*-[PtMe(CH=CH$_2$)(MeNC)$_2$].** To a stirred solution of $[PtMe(Cl)(SMe_2)_2]$ (0.16 g, 0.32 mmol) in diethyl ether (10 mL) at −78 °C and under nitrogen was added a solution of vinylmagnesium bromide (1 mL of 1 M solution in THF) and the mixture was slowly brought to 0 °C. Excess Grignard reagent was destroyed by careful addition of a mixture of ether (5 mL) and water (0.1 mL). The solution was dried over anhydrous magnesium sulfate and filtered under nitrogen. To the filtrate at −40 °C was added dropwise a solution of MeNC (0.04 mL, 0.74 mmol) in diethyl ether (5 mL); the solution immediately became colorless. Removal of the solvent in vacuo at 0 °C resulted in a white solid product in 40% yield. NMR for *cis*-$[H^3H^2C{=}CH^1Pt(Me)(MeNC)_2]$ in acetone-d^6: δ (^1H) 6.85 [dd, H^1, $^3J(H^2)$ = 12, $^3J(H^3)$ = 19, $^2J(Pt)$ = 29 Hz], 5.83 [dd, H^2, $^3J(H^1)$ = 12, $^2J(H^3)$ = 5, $^3J(Pt)$ = 146 Hz], 5.27 [dd, H^3, $^3J(H^1)$ = 19, $^3J(H^2)$ = 5, $^3J(Pt)$ = 91 Hz], 0.35 [s, CH_3Pt, $^2J(Pt)$ = 74 Hz], 3.35 [m, CH_3NC, $^2J(NH)$ = 6 Hz], 3.43 [m, CH_3NC, $^2J(NH)$ = 6 Hz].

***cis*-[PtMe(CH$_2$CH=CH$_2$)(MeNC)$_2$].** This was prepared similarly from allylmagnesium bromide (1 mL of 0.8 M solution in ether) and $[PtMe(Cl)(SMe_2)_2]$ (0.11 g, 0.30 mmol) in diethyl ether (10 mL) and then addition of MeNC (0.05 mL, 0.92 mmol) in diethyl ether (5 mL). The yield of *cis*-$[PtMe(CH_2CH{=}CH_2)(MeNC)_2]$ was 0.087 g (87%). Anal. Calcd for $C_8H_{14}N_2Pt$: C, 28.8; H, 4.2; N, 8.4. Found: C, 28.7; H, 4.2, N, 8.0. NMR for *cis*-$[H^4H^3C^3{=}C^2H^5C^1H^2H^1PtMe(MeNC)_2]$ in CD_2Cl_2: δ (^1H) 1.95

(5) (a) Puddephatt, R. J.; Treurnicht, I. *J. Organomet. Chem.* **1987**, *319*, 129. (b) Kumar, R.; Roy, S.; Rashidi, M.; Puddephatt, R. J. *Polyhedron* **1989**, *8*, 551. (c) Kumar, R.; Puddephatt, R. J. *Can. J. Chem.*, in press. (d) Etspuler, A.; Suhr, H. *Appl. Phys.* **1989**, *A48*, 373. (e) Feurer, E.; Suhr, H. *Thin Solid Films* **1988**, *157*, 81. (f) Oehr, C.; Suhr, H. *Appl. Phys.* **1988**, *A45*, 151. (g) Baum, T. H. *Mater. Res. Soc. Symp. Proc.* **1987**, *75*, 141. (h) Gladfelter, W. L.; Boyd, D. C.; Hwang, J.-W.; Haasch, R. T.; Evans, J. F.; Ho, K. L.; Jensen, K. F. In ref 1b, p 447. (i) Beach, D. B.; Legoues, F. K.; Hu, C. K. *Chem. Mater.* **1990**, *2*, 216.

(6) Westwood, W. *Gmelin Handbook of Inorganic Chemistry—Supplement Vol. A1*; 1986; pp 43–50 and references therein.

(7) Xue, Z.; Strouse, M. J.; Shuh, D. K.; Knobler, C. B.; Kaesz, H. D.; Hicks, R. F.; Williams, R. S. *J. Am. Chem. Soc.* **1989**, *111*, 8779 and references therein.

(8) (a) Roy, S.; Puddephatt, R. J.; Scott, J. D. *J. Chem. Soc., Dalton Trans.* **1989**, 2121. (b) Clark, H. C.; Manzer, L. E. *J. Organomet. Chem.* **1973**, *59*, 411.

(9) (a) Carturan, G.; Scrivanti, A.; Belluco, U. *Inorg. Chem. Acta* **1977**, *21*, 103. (b) Boag, N. M.; Green, M.; Spencer, J. L.; Stone, F. G. A. *J. Chem. Soc., Dalton Trans.* **1980**, 1200; **1980**, 1208.

[d, H^1H^2, $^3J(H^5)$ = 8, ^2J(Pt) = 101 Hz], 4.52 [tdd, H^3, $^4J(H^1H^2)$ = 1, $^2J(H^4)$ = 3, $^3J(H^5)$ = 17, ^4J(Pt) = 30 Hz], 34.24 [tdd, H^4, $^4J(H^1H^2)$ = 1, $^2J(H^3)$ = 3, $^3J(H^5)$ = 10, ^4J(Pt) = 29 Hz], 5.92 [ddt, H^5, $^3J(H^1H^2)$ = 8, $^3J(H^3)$ = 17, $^3J(H^4)$ = 10 Hz], 0.20 [s, CH_3Pt, ^2J(Pt) = 74 Hz], 3.11 [m, CH_3NC, ^2J(NH) = 6 Hz], 3.15 [m, CH_3NC, ^2J(NH) = 6 Hz]. δ (^{13}C) 26.9 [^1J(PtC) = 571 Hz, C^1], 147.4 [^2J(PtC) = 60 Hz, C^2], 104.3 [^3J(PtC) = 62 Hz, C^3], -7.5 [^1J(PtC) = 599 Hz, PtMe], 29.5, 29.6 [CH_3CN]. MS, m/e = 333 (M), 319 (M - CH_2).

The complexes *cis*-[PtMe(CH_2CH=CH_2)(2,6-Me_2-$C_6H_3NC)_2$] [Anal. Calcd for $C_{22}H_{26}N_2$Pt: C, 51.4; H, 5.1; N, 5.4. Found: C, 50.9; H, 4.9, N, 5.4. NMR for *cis*-[$H^4H^3C^3$=$C^2H^5C^1H^2H^1$PtMe-(XyNC)$_2$] in CD_2Cl_2: δ (^{1}H) 4.77 [tdd, H^3, $^4J(H^1H^2)$1, $^2J(H^4)$ = 3, $^3J(H^5)$ = 17, ^4J(Pt) = 29 Hz], 4.44 [tdd, H^4, $^4J(H^1H^2)$ = 1, $^2J(H^3)$ 3, $^3J(H^5)$ = 10, ^4J(Pt) = 27 Hz], 6.15 [ddt, H^5, $^3J(H^1H^2)$ = 8, $^3J(H^3)$ = 17, $^3J(H^4)$ = 10 Hz], 0.69 [s, CH_3Pt, ^2J(Pt) = 74 Hz], 2.43-2.44 [s, 12 H, 2,6-(CH_3)$_2C_6H_3$], 7.11, 7.15, 7.22 [s, 6H, C_6H_3]. δ (^{13}C) 22.5 [^1J(PtC) = 568 Hz, C^1], 146.7 [^2J(PtC) = 60 Hz, C^2], 105.4 [^3J(PtC) = 64 Hz, C^3], -5.7 [^1J(PtC) = 591 Hz, PtMe]. MS, m/e = 513 (M), 498 (M - CH_3), 472 (M - allyl), 367 (M - CH_3 - XyNC)] and [PtMe(CH_2CH=CH_2)(^{t}BuNC)$_2$] [Anal. Calcd for $C_{12}H_{26}N_2$Pt: C, 36.6; H, 6.7; N, 7.1. Found: C, 36.6; H, 6.6; N, 6.9. NMR for *cis*-[$H^4H^3C^3$=$C^2H^5C^1H^2H^1$PtMe (*t*-BuNC)$_2$]: δ (^{1}H) 2.78 [d, H^1H^2, $^3J(H^5)$ = 8, ^2J(Pt) = 101 Hz], 5.28 [m, H^3, $^2J(H^4)$ = 3, $^3J(H^5)$ = 17 Hz], 5.01 [tdd, $^4J(H^1H^2)$ = 1, $^2J(H^3)$ = 3, $^3J(H^5)$ = 9 Hz], 6.46 [ddt, H^5, $^3J(H^1,H^2)$ = 8, $^3J(H^3)$ = 17, $^3J(H^4)$ = 9 Hz], 1.05 [s, CH_3Pt, ^2J(Pt) = 74 Hz], 2.28 [s, 18 H, *t*-Bu]. δ (^{13}C) 21.4 [^1J(PtC) = 568 Hz, C^1], 147.5 [^2J(PtC) = 63 Hz, C^2], 104.2 [^3J(PtC) = 60 Hz, C^3], -7.2 [^1J(PtC) = 596 Hz, PtMe], (30.5, 30.4) [*t*-Bu]. MS, m/e = 417 (M), 376 (M - allyl)] were prepared in a similar way and were isolated in 92 and 71% yields, respectively.

[PtMe(CH_2CH=CH_2)(COD)]. To a stirred solution of [PtMe(Cl)(COD)] (0.33 g, 0.93 mmol) in diethyl ether (20 mL) at -78 °C and under nitrogen was added dropwise a solution of allylmagnesium bromide (2 mL of 0.8 M solution) in ether. After this was stirred for 3 h at 0 °C, excess Grignard reagent was destroyed by adding water (0.1 mL). The solution was dried over magnesium sulfate and filtered, and solvent removed at 0 °C to leave behind a yellow solid, which was washed with cold pentane and dried in vacuo (yield 0.19 g, 56%). Anal. Calcd for $C_{12}H_{20}$Pt: C, 40.1; H, 5.6. Found: C, 39.8; H, 5.6. NMR for [H^4H^3C=$CH^5CH^1H^2$PtMe(COD)] in CD_2Cl_2: δ (^{1}H) 2.27 [d, H^1H^2, $^3J(H^5)$ = 9, ^2J(Pt) = 115 Hz], 4.45 [dd, H^4, $^2J(H^3)$ = 3, $^3J(H^5)$ = 11, ^4J(Pt) = 32 Hz], 5.94 [ddt, H^5, $^3J(H^1H^2)$ = 9, $^3J(H^3)$ = 16, $^3J(H^4)$ = 11 Hz], 4.6-4.8 [m, 4 H, J(Pt) = 42 Hz, -HC=CH-], 2.1-2.4 [m, 8 H, (CH_2CH_2)], 0.67 [s, CH_3Pt, ^2J(Pt) = 82 Hz]. MS, m/e = 359 (M), 345 (M - CH_2), 318, (M - allyl).

[PtMe(C≡C^{t}Bu)(MeNC)$_2$]. To a stirred solution of [PtMe(Cl)(SMe_2)$_2$] (0.12 g, 0.31 mmol) in diethyl ether (10 mL) at -78 °C and under nitrogen was added dropwise an ether solution of (*tert*-butylethynyl)lithium (0.9 mmol in 10 mL) from above. The mixture was slowly brought to 0 °C, after which excess organolithium reagent was destroyed by the addition of water (0.1 mL). The ether layer was dried over magnesium sulfate and filtered. To the filtrate was added a solution of MeNC (0.06 mL, 1.1 mmol) in diethyl ether (5 mL) at -78 °C, and the product was isolated as described above. It was crystallized from benzene/hexane. The yield of [PtMe(C≡C^{t}Bu)(MeNC)$_2$] was 0.61 g (49%). Anal. Calcd for $C_{11}H_{18}N_2$Pt: C, 35.4; H, 4.9; N, 7.5. Found: C, 35.0; H, 4.6; N, 7.4. NMR in C_6D_6: δ (^{1}H) 1.53 [s, 9 H, ^{t}Bu], 1.48 [s, ^2J(Pt) = 68 Hz, PtMe], 1.83 [s, ^2J(NH) = 10 Hz, CNMe], 2.0 [s, ^2J(NH) = 12 CN*Me*]. MS, m/e = 373 (M), 358 (M - CH_3), 292 (M - BuCC).

Thermolysis of the CVD Precursors. Solid-state decomposition of the precursor (0.1 mmol) was carried out by gently heating to the decomposition temperature. The condensible volatile products were collected at liquid nitrogen temperature, and the total gas mixture was subjected to GC and GC-MS analysis. The involatile products were extracted with ether, hexane, or dichloromethane, filtered through a Florisil pad, and subjected to GC-MS study.

In a typical gas-phase thermolysis experiment, 2 mg (6.5×10^{-3} mmol) of the precursor was completely vaporized inside the IR gas cell at 480 K. The temperature of the cell was then increased to 580 K within 5 min, and the decomposition was monitored by IR until completion. The temperature of the IR window was slightly lower than that at the central part of the cell, and hence decomposition occurred largely in the cell center and negligible deposition of metallic platinum on the KCl window occurred. The progress of the reaction was monitored by the slow disappearance of the ν(C≡N) peaks at 2195 and 2216 cm^{-1} and the appearance of signals at 3017 and 1305 cm^{-1}. The latter two peaks are due to methane, as confirmed by recording the spectrum of pure methane.

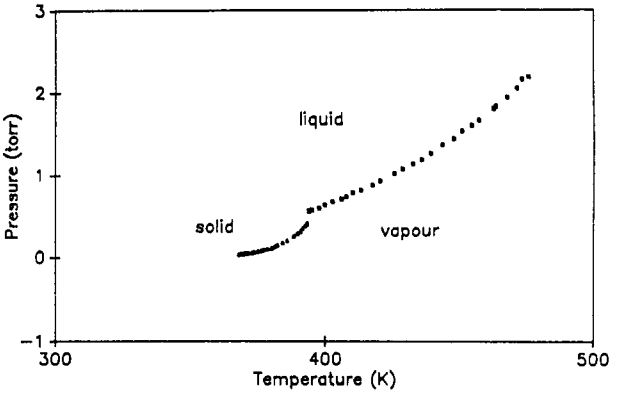

Figure 1. Vapor pressure of *cis*-[$PtMe_2$(MeNC)$_2$] as a function of temperature.

Vapor Pressure of *cis*-[$PtMe_2$(MeNC)$_2$] (1). This was determined by measurement of the IR absorbance at 2200 cm^{-1} [ν(NC)] of a known mass of the complex in the IR cell as a function of temperature. A plot of ln [A(2200)] vs $1/T$ (Clausius-Clapeyron plot, assuming Beer-Lambert law) then gave three intersecting straight lines corresponding to situations with solid-gas equilibrium, liquid-gas equilibrium, and gas phase only present, respectively, as the temperature was raised. From the high-temperature region, where all complex was in the gas phase, the pressure of 1 could be calculated by using the ideal gas law, and hence the pressure-absorbance relationship was determined. The phase diagram shown in Figure 1 was then derived. The vapor pressure of 1 at 25 °C was 3.3×10^{-6} Torr. This is considerably lower than the vapor pressure of [Pt(C_5H_4Me)Me_3], which is 5.3×10^{-2} Torr at 23 °C.[7]

Results and Discussion

Synthesis of New Precursors. The following complexes have been synthesized for the present study: *cis*-[$PtMe_2$(MeNC)$_2$] (**1**), *cis*-[Pt(CD_3)$_2$(MeNC)$_2$] (**2a**), *cis*-[$PtMe_2$(CD_3NC)$_2$] (**2b**), *cis*-[$PtMe_2$(XyNC)$_2$] (**3**, Xy = 2,6-$Me_2C_6H_3$), [$PtMe_2$(COD)] **4**, COD = 1,5-cyclooctadiene), *cis*-[PtMe(σ-CH_2CH=CH_2)(MeNC)$_2$] (**5**), *cis*-[PtMe(σ-CH_2CH=CH_2)(XyNC)$_2$] (**6**), *cis*- [PtMe(σ-CH_2CH=CH_2)(^{t}BuNC)$_2$] (**7**), [PtMe(σ-CH_2CH=CH_2)-(COD)] (**8**), *cis*-[PtMe(CH=CH_2)(MeNC)$_2$] (**9**), and [PtMe(^{t}BuC≡C)(MeNC)$_2$] (**10**). Complexes **1-4** were prepared by literature methods.[8] The new complexes **5-7**, **9**, and **10** were prepared by the following general route (eq 1), in which an excess of organolithium or Grignard reagent

$$\textit{trans}\text{-[PtClMe(SMe}_2)_2] \xrightarrow[-\text{MgXCl/LiCl}]{\text{RMgX/RLi}} \textit{cis}\text{-[PtMeR(SMe}_2)_2] \xrightarrow[-2\text{SMe}_2]{+2\text{R'NC}} \text{[PtMeR(R'NC)}_2] \quad (1)$$

was added to a solution of *trans*-[$PtClMe(SMe_2)_2$] in diethyl ether at -78 °C to give *cis*-[$PtMeR(SMe_2)_2$], which was isolated only as a solution in ether at 0 °C. Addition of the isocyanide ligand to the solution of *cis*-[$PtMeR(SMe_2)_2$] afforded the compounds [$PtMeR(R'NC)_2$] in moderate yields. All efforts to isolate complexes *cis*-[$PtMeR(SMe_2)_2$], when R was not methyl, in pure form were unsuccessful. Attempts to synthesize an unsymmetrical organoplatinum(II) complex having a η^3-allyl group by the addition of 1 mol equiv of organic isocyanide to *cis*-[PtMe(CH_2CH=CH_2)(SMe_2)$_2$] resulted in the forma-

Table I. Gas-Phase IR Spectra (cm^{-1}) of Organometallic Precursors and MeNC

compound	ν(CH)	ν(N≡C)	other
$[PtMe_2(MeNC)_2]$	2917, 2874, 2806	2216, 2195	1423, 1408, 1219, 1054, 1027, 973
$[Pt(CD_3)_2(MeNC)_2]$	2928, 2854	2218, 2197	1409, 1041, 1036, 2102, 2052 [ν(CD)]
$[PtMe_2(CD_3NC)_2]$	2917, 2876, 2806	2218, 2195	2111 [ν(CD)]
[PtMe(allyl)$(MeNC)_2$]	3087, 2953, 2923, 2874, 2857, 2809	2218, 2195, 2213, 2184, 2073	2111 [ν(CD)]
[PtMe(vinyl)$(MeNC)_2$]	3086, 3017, 2917, 2876, 2809	2218, 2197	1605 [ν(C=C)]
$[PtMe(^tBuC{\equiv}C)(MeNC)_2]$	2963, 2928, 2874	2221, 2195	
[$PtMe_2$(COD)]	3017, 2952, 2928, 2897, 2855	2221, 2195	
MeNC	2977, 2953	2175, 2150	

tion of *cis*-$[PtMe(CH_2CH{=}CH_2)(RNC)_2]$ along with uncharacterized decomposition product(s). Attempts to prepare the complexes from *trans*-$[PtClMe(SMe_2)_2]$ by the addition of R'NC followed by RLi or RMgBr were also unsuccessful. Compound **8** was prepared from *cis*-[PtClMe(COD)] and allylmagnesium bromide at −78 °C.

The precursors are colorless or pale-yellow solids except for **7**, which is an oil. The thermal stability of the compounds varies depending on the ligands. For example, compounds **1–4** are air stable, **5**, **6**, and **8–10** can be stored indefinitely at 0 °C in the absence of light, and **7** decomposes slowly at 0 °C.

The choice of isocyanide as supporting ligand was based on the usefulness of the N≡C stretching mode in the IR for monitoring reactions and on the successful use of [MeAu(MeNC)] as a precursor for CVD of gold.[5a]

Gas-Phase IR Spectra of Organometallic Precursors. The gas-phase spectra of the CVD precursors have also been recorded by using a heated 10-cm gas cell fitted with KCl windows. With the exception of *cis*-$[PtMe(CH{=}CH_2)(MeNC)_2]$, the compounds did not decompose below 150 °C, and spectra could be recorded until a solid–vapor/liquid–vapor equilibrium was reached. The ν(CH), ν(N≡C), and other selected peaks for the compounds are shown in Table I. Detailed group frequency analysis has not been attempted; however, the following qualitative observations can be made:

(i) Complexes having coordinated isocyanide ligand show two well-defined peaks at ~2200 cm^{-1} due to the symmetric and asymmetric C≡N stretching modes. These peaks appear from 40 to 45 cm^{-1} to higher wavenumber compared to the ν(NC) stretching frequencies of the free ligand MeNC.

(ii) The C–H vibrational stretches appear in the 2800–3000-cm^{-1} region. For example, *cis*-$[PtMe_2(MeNC)_2]$ has $\nu(CH_3Pt)$ = 2874 and 2806 cm^{-1} and $\nu(CH_3N)$ = 2917 and 2874 cm^{-1}, with the 2874-cm^{-1} band having components from both types of methyl group. This assignment was readily confirmed by recording the spectrum of *cis*-$[Pt(CD_3)_3(MeNC)_2]$; the C–D stretching frequencies appear at 2102 and 2052 cm^{-1}, in good agreement with the calculated values (2109 and 2059 cm^{-1}), while the $\nu(CH_3N)$ bands were at 2928 and 2854 cm^{-1}. The slight frequency shifts compared to **1** are probably due to some coupling of vibrational modes. However, *cis*-$[PtMe_2(CD_3NC)_2]$ gave three C–H stretching peaks although NMR analysis showed that there was little H impurity in the CD_3NC groups; the C–D stretch was at 2111 cm^{-1} (calcd 2110 cm^{-1}), and the expected second such peak (calcd 2141 cm^{-1}) was obscured by the much stronger ν(CN) stretch.

(iii) The spectrum of the vinyl complex *cis*-$[PtMe(CH{=}CH_2)(MeNC)_2]$ shows a peak at 1605 cm^{-1}, due to the C=C stretching vibration.

The CVD Experiment. The chemical vapor deposition of platinum films on a silicon substrate was carried out by using a vertical Pyrex reactor, under dynamic pumping at a pressure of 2×10^{-3} Torr and at 200–250 °C, the precursor being heated in some cases to 30–80 °C to increase the vapor pressure and hence afford more rapid deposition. CVD was also carried out successfully by using a horizontal reactor and glass, copper, or metal alloy substrates. The substrate could be heated electrically or, with a quartz reactor, by infrared, or (when the ligand was MeNC but not 1,5-cyclooctadiene) by UV irradiation. With the equipment used, the maximum temperature attainable with UV heating was approximately 150 °C, and since thermolysis of **1** does not occur at this temperature, the CVD is clearly photochemically enhanced when the ligand is MeNC. In all cases, the deposition temperature could be lowered to 100–150 °C when CVD was carried out in the presence of hydrogen. The allylplatinum complex *cis*-$[PtMe(CH_2CH{=}CH_2)(MeNC)_2]$ gave efficient CVD at 180 °C, whereas the complex *cis*-$[PtMe_2(MeNC)_2]$ required 250 °C for efficient CVD. Thus the σ-allyl group provides a weak link and allows CVD at a significantly lower temperature, presumably due to the lower Pt-C bond energy for the allyl–platinum compared to the methyl–platinum group. The vinyl derivative also decomposed at lower temperature, but its synthesis is more difficult and it decomposes on storage, so it has not been examined in as much detail.

Measurement of the thickness of platinum films coated on glass substrates at 250 °C using *cis*-$[PtMe_2(MeNC)_2]$ as CVD precursor indicates a linear dependence of film thickness with deposition time, the rate of film growth being 100 ± 15 Å/min.

The conductance of the film, measured by the four-point probe method, gives a value of $(1.4–3.0) \times 10^4$ mho cm^{-1}, which is lower than the bulk platinum value (99.8% pure Pt has a conductivity of 9.4×10^4 mho cm^{-1}) but still indicates that these films are of high metallic quality. The films have a thickness of 50 nm or more and thus are above the limit (8–12.5 nm) where resistivity depends on film thickness.[10]

The morphology of the films was studied by scanning electron microscopy (Figure 2). Films deposited in the presence of hydrogen have smoother surfaces with fine-grain boundaries (crystallite size ca. 500 Å), whereas films deposited in the absence of hydrogen have a coarser surface (crystallite size ca. 2000 Å).

Composition of Films. The films were analyzed by XPS, and the analytical data are shown in Table II. The effect of argon ion sputtering and the hydrogen flow rate on the purity of the films was also studied and is described below, using films prepared from *cis*-$[PtMe_2(MeNC)_2]$ as an example (Table III). Other precursors gave very similar results.

All the films show the presence of carbon (and often oxygen) as impurities. The carbon impurities on the surface arise both from the CVD process itself and from subsequent exposure to the atmosphere. Thus, a freshly prepared film, analyzed by XPS and then exposed to laboratory atmosphere for 5 h, shows considerable increase

(10) Angadi, A.; Shivaprasad, S. M. *J. Mater. Sci.* **1984**, *19*, 2396.

Table II. Analytical Data for Platinum Films

compound	H_2 present	XPS anal.,[a] % Pt	C	O
$[PtMe_2(MeNC)_2]$	no	88	11	
	yes	95	5	
$[PtMe_2(COD)]$	no	86	10	4
	yes	94	4	2
$[PtMe(\sigma\text{-allyl})(MeNC)_2]$	no	86	10	4
	yes	96	4	
$[PtMe(\sigma\text{-allyl})(COD)]$	no	61	37	2
	yes	94	4	2
$[PtMe(vinyl)(MeNC)_2]$	no	72	28	
	yes	82	15	3
$[PtMe(^tBuC{\equiv}C)(MeNC)_2]$	no	56	31	13
	yes	70	21	9
$[PtMe(\eta^1\text{-}C_5H_5)(COD)]$	no	77	19	4
	yes	95	5	
$[PtMe(\eta^5\text{-}C_5H_5)(CO)]$	no	71	27	2
	yes	93	4	3
$[PtMe_3(\eta^5\text{-}C_5H_5)]$	no	74	25	1
	yes	94	6	
$[PtMe_3(acac)]_2$	no	66	30	4
	yes	89	6	5
$[Pt(\eta^3\text{-}C_3H_5)(\eta^5\text{-}C_5H_5)]$	no	60	38	2
	yes	95	5	

[a] After 30 s of Ar ion sputtering.

Table III. XPS Analytical Data for Films Prepared from $[PtMe_2(MeNC)_2]$

H_2 flow rate, mL min^{-1}	sputter time, s	atom % Pt	C	O
0	15	64	34	1
20	15	87	11	2
40	15	94	4	2
100	15	94	4	2
40	0	87	11	2
40	15	94	4	2
40	30	96	2	2
40	60	100	0	0
40[a]	a	52	39	9

[a] Above sample exposed to atmosphere for 10 min and then reanalyzed. No additional sputtering.

in the carbon percentage. However, upon sputtering, the carbon percentage decreases very rapidly with sputter depth and approaches its original value. A 60-s sputtering to give a pure platinum film followed by 10-min laboratory exposure leads to carbon analysis of about 40% on the film surface. Hence XPS analyses were carried out after argon ion sputtering for 30–60 s to remove the surface contamination.

The carbon content decreased considerably for films prepared with hydrogen as carrier gas, while still maintaining dynamic pumping. From a study on hydrogen flow rate vs composition it can be concluded that most impurities were removed at a flow rate of 20 mL min^{-1} through the apparatus, and the film purity then improved only slightly at higher flow rates. A film prepared under hydrogen and only briefly exposed to laboratory atmosphere gave a high platinum purity on the surface, and upon sputtering for 60 s, 100% pure platinum was present and no carbon or oxygen impurities were detected.

The above results show that the carbon deposition on the surface of an exposed film mostly originates from the atmosphere, that the carbon in the sublayers arises from the CVD process, that the concentration of these impurities also appears higher near the surface, and that CVD under hydrogen definitely reduces the carbon content in the sublayers.

Nature of Carbon Impurities in the Platinum Film. Narrow-scan XPS analysis was carried out in the 275–295 (C(1s)) and 65–85 (Pt(4f)) eV regions, of two films prepared

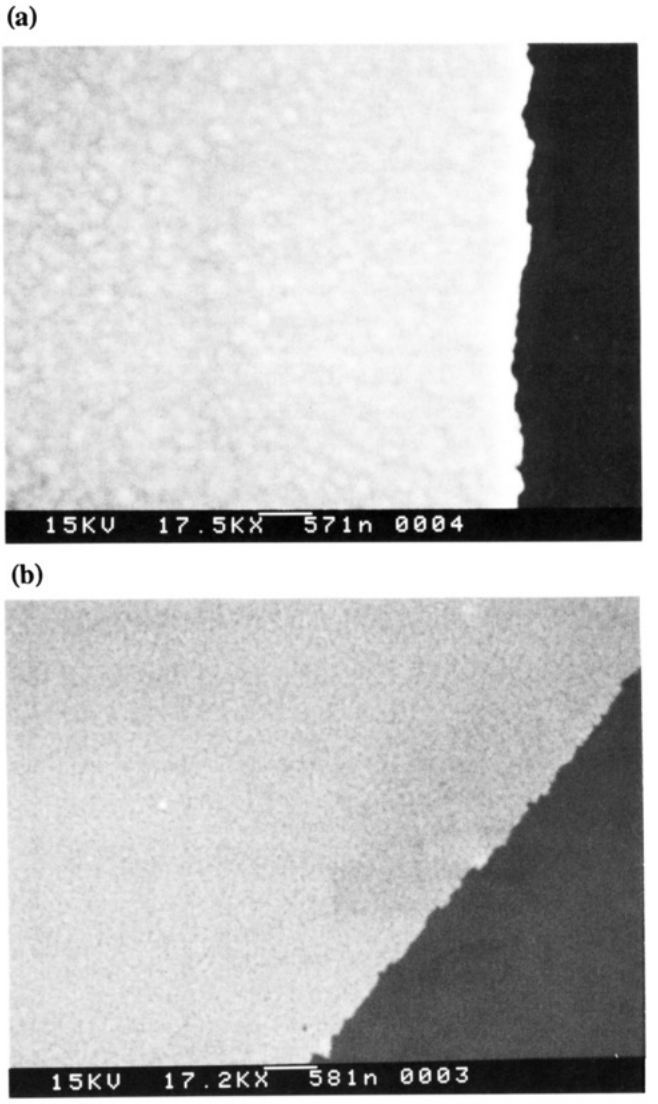

Figure 2. Scanning electron microscopy of platinum films formed from *cis*-$[PtMe_2(MeNC)_2]$: (a) without hydrogen carrier gas, grain size ca. 2000 Å; (b) with hydrogen carrier-gas, grain size ca. 500 Å.

by CVD without hydrogen using the precursors $[PtMe_2(MeNC)_2]$ and $[Pt(CD_3)_2(MeNC)_2]$, respectively (Figure 3). The films were deposited on silicon substrates. Under these conditions sufficient carbon impurities were present to allow detailed study. The films were exposed to the atmosphere for a minimum time and were briefly sputtered before XPS analysis to minimize the presence of atmospheric carbon interference. The C(1s) binding energy region showed three peaks at nearly the same positions for both films. The main peak appears at 283.9–284.1 eV, while two other peaks appear at 283.1–283.7 and 285.9–286.0 eV, respectively. Carbon fragments that give signals in the 284-eV region are carbide, graphite, and hydrocarbons,[11] and the XPS data cannot easily distinguish between these. The higher binding energy peak is likely to be due to C–O groups.[11] The platinum $4f_{5/2}$ and $4f_{7/2}$ peaks appear consistently at 74.4–74.5 and 71.0–71.1 eV, respectively, as expected for metallic platinum, and there were no secondary peaks (in parts B and D of Figure 3, the poor fit on the high binding energy side is due to

(11) (a) Gelius, U.; Heden, P. F.; Hedman, J.; Lindberg, B. J.; Manne, R.; Nordberg, R.; Nordling, C.; Siegbahn, K. *Phys. Scr.* **1970**, *2*, 70. (b) Morgen, P.; Szymonski, M.; Onsgaard, J.; Jorgensen, B.; Rossi, G. *Surf. Sci.* **1988**, *197*, 347.

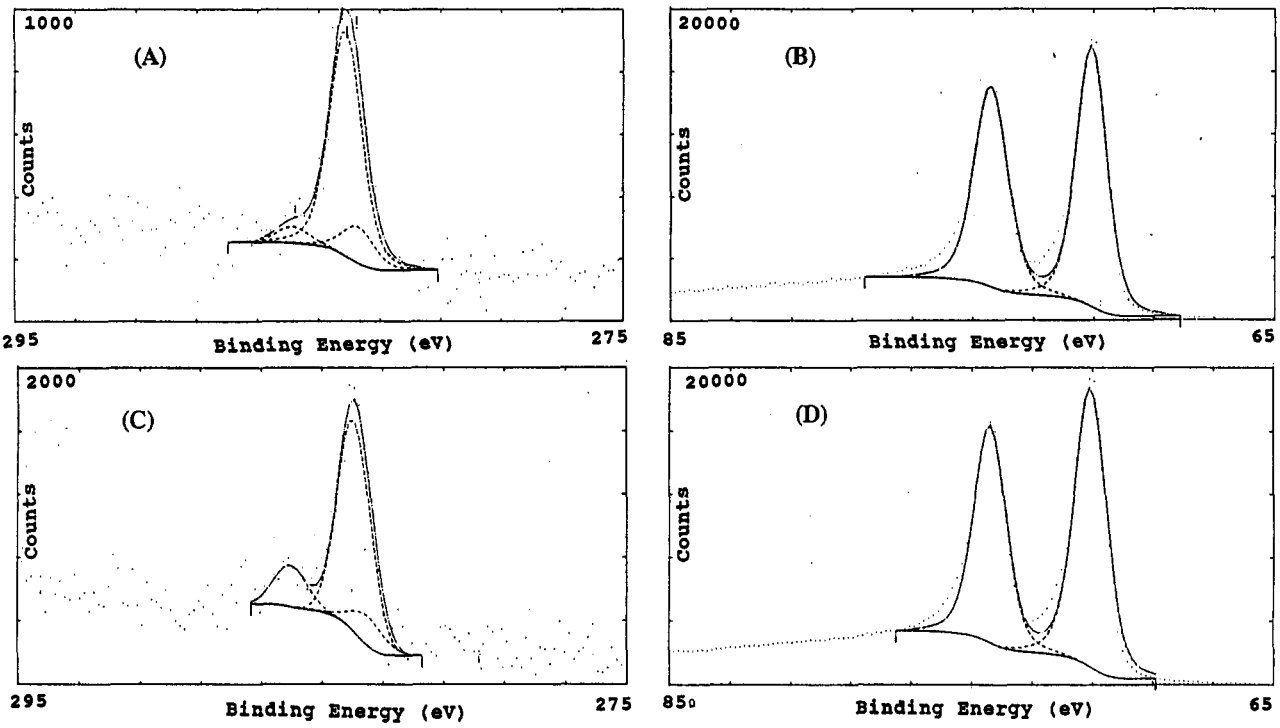

Figure 3. Narrow-scan XPS analysis of platinum films formed by CVD from *cis*-$[PtMe_2(MeNC)_2]$ (A, C(1s) region; B, Pt(4f) region) and *cis*-$[Pt(CD_3)_2(MeNC)_2]$ (C, C(1s) region; D, Pt(4f) region) in the absence of hydrogen. Conditions correspond to the first entry in Table III.

Table IV. Composition of Organic Products from the Thermolysis of CVD Precursors *cis*-$[PtMeRL_2]$

R	L	conditions[a]	temp, °C	hydrocarbon[b]	other[c]
Me	MeNC	s	180	CH_4 (78‰), C_2H_6 (22%)	MeNC (trace)[d]
Me	MeNC	g	250	CH_4 (100%)	*d*
Me	MeNC	s + H_2	180	CH_4 (100%)	MeNC[d]
Me	MeNC	g + D_2	200	CH_3D (100%)[e]	*d*
Me	XyNC	s	200	CH_4 (76%), C_2H_6 (24%)	$XyNH_2$, $XyN{=}CMe_2$[f]
Me	COD	s	180	CH_4 (100%)	C_8H_{12}
vinyl	MeNC	s	150	CH_4 (27%), C_4H_6 (63%)	MeNC[d]
allyl	MeNC	s	180	CH_4 (75%), C_3H_6 (6%), C_6H_{10} (19%)	MeNC[d]
allyl	XyNC	s	200	CH_4 (75%), C_3H_6 (5%), C_6H_{10} (20%)	$XyNH_2$, $XyN{=}CMe_2$[g]

[a] s = solid; g = gas; + H_2 = hydrogen present; + D_2 = deuterium present. [b] Products identified independently by GC and GC-MS. C_3H_6 = propene; C_4H_6 = 1,3-butadiene; C_6H_{10} = 1,5-hexadiene; C_8H_{12} = cyclooctadiene. Relative yields determined by GC. [c] Volatile products identified by GC-MS but relative yields not determined. [d] Most MeNC incorporated in an involatile polymer, not detected by GC. [e] MS analysis confirmed the product to be CH_3D; calcd mass for CH_3D 17.0376, found 17.0379. [f] 56:44 ratio. [g] 40:60 ratio.

the inappropriate fitting function and the shakeup resulting from the high density of states at the Pt Fermi level).

The films from the XPS analysis above were subjected further to a SIMS depth profile study, which was carried out using Cs^+ as primary ion (ion current <100 nA). Secondary ions at mass numbers 1, 2, 12, 13, 14, 15, 16, 18, 30, and 195 were monitored as a function of time. The following observations were made from six independent experiments: (i) Well-defined interface characteristics were seen in all cases; that is, there was a sharp transition from platinum-rich to silicon-rich phases.[11] (ii) The carbon impurities decreased but were still detectable in the silicon phase. (iii) Films prepared from $[Pt(CD_3)_2(MeNC)_2]$ showed very high count rates at $m/e = 2$ (the deuterium signal) whose intensity parallelled that of the platinum signal (at $m/e = 195$) very well along the film depth; subsequently both the signals fell when the Si signal (at $m/e = 30$) grew in intensity. (iv) The relative intensities of the peaks at $m/e = 13$ and 14, corresponding in part to CH and CD, respectively, were consistently higher throughout the platinum-rich region for films prepared from the CH_3Pt [$I_{13}/I_{14} = 26 \pm 4$] compared to the CD_3Pt [$I_{13}/I_{14} = 5 \pm 3$] precursor. Since other contributing ions, such as nitrogen at $m/e = 14$, are likely to be constant in all samples, the presence of CH is higher in films prepared from CH_3Pt precursor and CD is higher in films prepared from CD_3Pt precursor.[12] The results from iii and iv indicate that the carbon impurities arise, at least in part, from the methylplatinum groups and that some hydrocarbon as well as carbide is present. At present, the nature of the carbon impurities cannot be defined more fully.

Thermolysis of the Precursors. Understanding the mechanism and products of the thermolysis of the organometallic precursors is essential in developing the CVD process. Toward this end, attempts have been made to study the decomposition of the complexes in the solid state and in the gas phase by ex situ (GC, GC-MS, TG-FTIR, DSC) and in situ (FTIR) techniques, and the results are presented below.

Solid-State Decomposition of Organometallic Precursors. The complexes were heated to complete de-

(12) (a) Kaminsky, M. K.; Winograd, N.; Geoffroy, G. L.; Vannice, M. A. *J. Am. Chem. Soc.* **1986**, *108*, 1315. (b) Collister, J. L.; Pritchard, H. O. *Can. J. Chem.* **1976**, *54*, 2380. From kinetic data given in this paper, the half life of MeNC at 250 °C can be estimated to be 3 min, which compares with our observation of 7 min.

composition in the absence of oxygen and the volatile products were collected on the vacuum line and subsequently analyzed by GC and GC-MS. The involatile products were analyzed by GC-MS, wherever possible. In the case of $[PtMe_2(MeNC)_2]$, the decomposition was also carried out in the gas-phase and in the presence of hydrogen. The major observations are described below (Table IV).

(i) *cis*-$[PtMe_2(MeNC)_2]$ (1) decomposed in the solid state at 180 °C, giving a mixture of methane and ethane in a 78:22 ratio. However, the decomposition in the gas phase or in the presence of hydrogen gave methane only. That hydrogen is indeed taking part in the reaction is evident from the exclusive formation of CH_3D during the decomposition of 1 in an atmosphere of deuterium. Dimethylplatinum(II) complexes 3 and 4 behave similarly.

(ii) The thermolysis of the mixed alkyl complexes $[PtR(Me)(R'NC)_2]$ where R is an allyl (compounds **5** and **6**) or vinyl group (compound **9**) resulted in the formation of significant amounts of intermolecular coupling products 1,5-hexadiene or 1,3-butadiene formed from allyl or vinyl groups, respectively, but no intramolecular coupling product 1-butene or propene by combination of methyl and allyl or vinyl group, respectively, was observed. Thus intramolecular reductive elimination does not occur.

(iii) The solid-state decomposition of compounds having MeNC as ligand gave the free ligand along with an involatile, apparently polymeric, product that was insoluble in most organic solvents.

(iv) In contrast, thermolysis of *cis*-$[PtMe_2(XyNC)_2]$, R = xylyl, gave an oil that was shown to be a mixture of $[2,6\text{-}Me_2C_6H_3NH_2]$ and $[2,6\text{-}Me_2C_6H_3N{=}C(Me_2)]$. The imine derivative is formed by combination of XyNC with two methylplatinum groups, and the amine is probably then formed by its hydrolysis.

IR Study of the Decomposition of $[PtMe_2(MeNC)_2]$ from the Vapor. Because the volatility and thermal stability were suitable, the compounds $[PtMe_2(MeNC)_2]$ (1), $[Pt(CD_3)_2(MeNC)_2]$ (**2a**), and $[PtMe_2(CD_3NC)_2]$ (**2b**) were chosen for study of thermolysis from the vapor by using FTIR. The precursor was completely vaporized without decomposition inside the evacuated gas cell at 207 °C, and the temperature of the cell was then rapidly increased to 307 °C. The decomposition was followed at this temperature by recording IR spectra as a function of time. The progress of the reaction was indicated by the slow disappearance of the $\nu(C{\equiv}N)$ peaks at 2195 and 2216 cm^{-1} due to 1 and by the appearance of peaks at 3017 and 1305 cm^{-1} due to methane.[12] Figure 4 represents a decay profile of the above decomposition in the range 1800–3200 cm^{-1}. It can be seen that two weak, broad peaks at 2232 and 2172 cm^{-1} also grew in. These peaks were still present after the cell was again evacuated and are due to an involatile, oily polymeric material that is probably formed from the methyl isocyanide ligands but that is not incorporated into the platinum films formed in a flow system. The decomposition of 1 and 2 was followed, as above, under various conditions. The results are summarized below.

Decomposition of 1 in the presence or absence of hydrogen and also in the presence or absence of free MeNC gave methane (3017-, 1305-cm^{-1} peaks)[12] as the only detectable hydrocarbon product. Decomposition of 1 in the presence of D_2 yielded exclusively the product CH_3D (3017-, 2199-, 1470-, 1303-, 1156-cm^{-1} peaks) with no detectable CH_4. This has also been confirmed by MS as described earlier. Free MeNC decomposed under the above conditions but did not yield methane; it isomerizes to MeCN under the reaction conditions.[12b] Hence the methane arises exclusively from the methylplatinum groups.

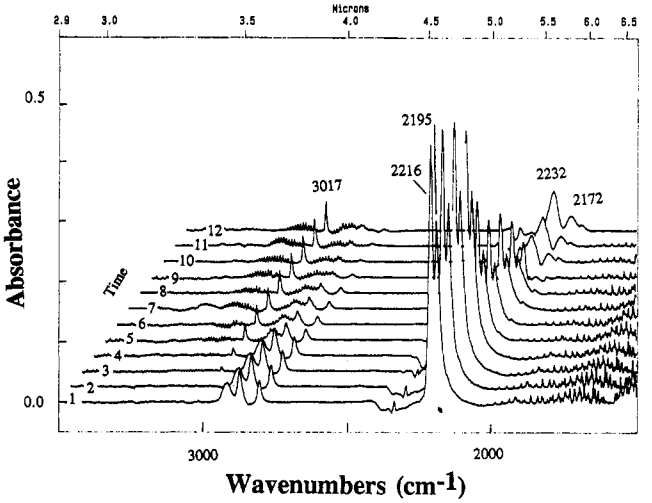

Figure 4. Changes the FTIR spectra during the gas-phase thermolysis of *cis*-$[PtMe_2(MeNC)_2]$. The peak labeled 3017 cm^{-1} is due to ν(CH) of product methane, those labeled 2216, 2195 cm^{-1} are due to ν(CN) of 1, and those labeled 2232, 2172 cm^{-1} are probably due to ν(CN) in the polymeric product.

The decomposition of **2a** in the absence of H_2 exclusively formed CD_3H (peaks at 2991, 2262, 2141, 1291, 1036, 1002 cm^{-1}), whereas in the presence of D_2 it gave CD_4 (peaks at 2257 and 994 cm^{-1}) plus a small amount of CD_3H (2991, 1036 cm^{-1}) but no CH_3D or CH_4 (3017 cm^{-1} absent). This again confirms that methane arises from methylplatinum groups and that the extra hydrogen atom required to give methane is not obtained from the other MePt group. Decomposition of **2b** gave CH_4 and no detectable CH_3D;[16] this shows that the extra hydrogen atom needed to form methane is not derived from the isocyanide ligand and hence, by elimination, that it is derived from adventitious hydrogen atoms, presumably on the cell walls.

The decomposition of **2a** was also carried out as above in an IR cell, the wall of which was partially deuterated by immersion of the cell in D_2O, *i*-PrOD, and NaOH solution followed by drying under vacuum, but this gave CD_3H and no CD_4. However, it is not known how effectively the SiOH groups in the cell wall were exchanged to give SiOD groups or how great the k_H/k_D isotope effect might be for abstraction of H/D by the methyl group, and so this experiment does not eliminate the possibility of hydrogen abstraction from the cell wall (surface reaction). Pyrolysis in the presence of hydrogen clearly gives methane by combination of a methylplatinum group with a hydrogen atom from H_2.

The gas-phase thermolysis was also carried out in the presence of free MeNC. Decomposition was negligible under the standard conditions until the MeNC decayed (by the known isomerization to give MeCN and probably, in part, by polymerization), and hence strong retardation by free ligand is proved. The IR peaks due to 1 were unchanged in the presence of the free MeNC, thus showing that no association occurred. Hence, the observation of retardation by free MeNC indicates that irreversible decomposition of $[PtMe_2(MeNC)_2]$ occurs after the reversible dissociation of a MeNC ligand from 1 to give an intermediate $[PtMe_2(MeNC)]$. The hydrocarbon product was methane.

The involatile product from the decomposition of 1 gave broad peaks at 2173 and 2230 cm^{-1}, and the corresponding peaks from **2a** appeared at 2171 and 2234 cm^{-1}; these are presumed due to $\nu(C{\equiv}N)$ in a polymeric material. In

Table V. TG-FTIR Analysis for the Decomposition of $[Me_2Pt(CNMe)_2]$ and $[Me_2Pt(COD)]$

compound	carrier gas[a]	temp, °C	wt loss, %	evolved gas[b]					
				CH_4	C_2H_6	MeNCO	CO_2	H_2O	L[c]
$[Me_2Pt(CNMe)_2]$	N_2	140–230	7.6	min	maj				tr
		250–380	11.6	maj	min	tr	tr		
		380–600	7.8	tr		min	maj	min	
		600–700	9.0				maj		
$[Me_2Pt(CNMe)_2]$	$N_2 + H_2$	140–210	8.0	maj	min				tr
		210–380	10.7	maj		tr	tr	min	*d*
		380–600	7.3			maj	maj	maj	
		600–720	9.7				maj		
$[Me_2Pt(CNMe)_2]$	$N_2 + O_2$	130–220	6.3	maj	maj	tr	tr		
		230–300	18.7	min		maj	maj		
		300–400	12.7				maj		
$[Me_2Pt(COD)]$	N_2	110–200	44.0	maj					maj
$[Me_2Pt(COD)]$	$N_2 + O_2$	110–220	42.3	maj			min	min	maj

[a] Gas flow rate = 100 mL min^{-1}; temperature ramp = 20 °C min^{-1}. [b] Detected by FTIR; maj = major or only product; min = minor product; tr = trace product. [c] L = MeNC or L_2 = COD. [d] Trace or $MeNH_2$ detected.

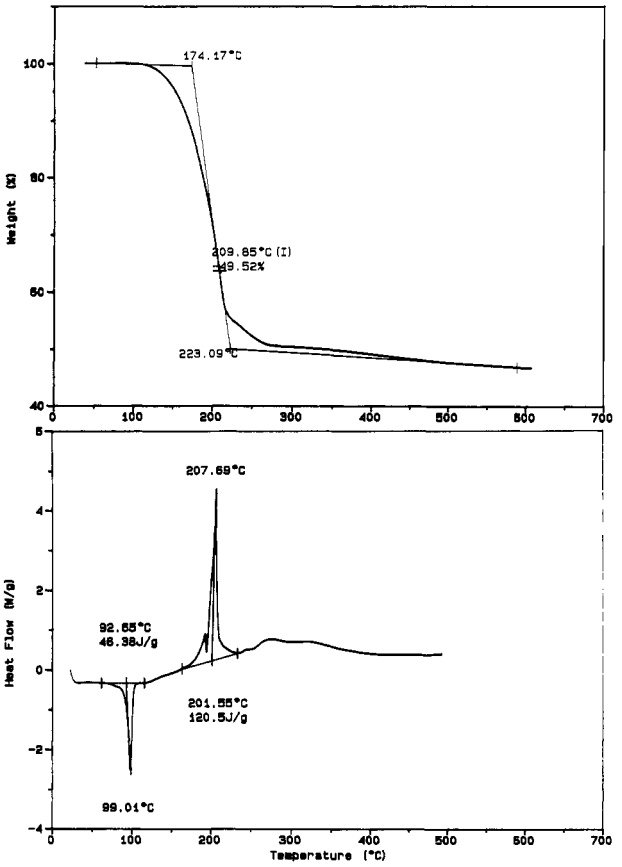

Figure 5. Top: thermogravimetric analysis (TGA) of the thermolysis of $[PtMe_2(COD)]$. Bottom: the corresponding differential scanning calorimetry (DSC) trace. The endotherm at 99 °C corresponds to melting, and the exotherm at 208 °C corresponds to thermolysis to metallic platinum.

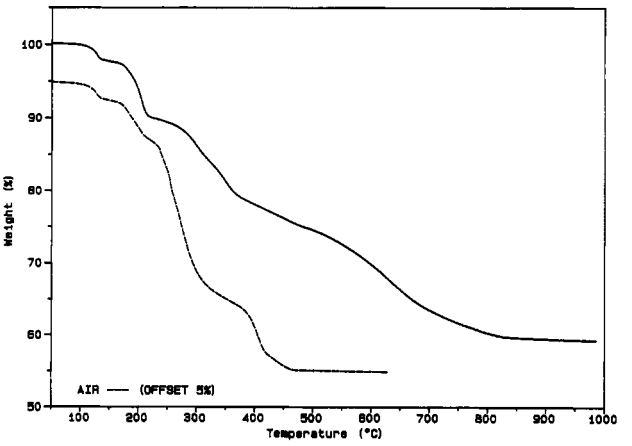

Figure 6. TGA traces for thermolysis of *cis*-$[PtMe_2(MeNC)_2]$: solid line, with N_2 carrier gas; dotted line, with N_2/O_2 carrier gas. In each case, the final weight loss corresponds to formation of metallic platinum.

contrast, the IR spectrum from the decomposition of free methyl isocyanide did not show any significant peaks in this region.

TGA-FTIR and DSC Studies. Differential scanning calorimetry (DSC) and thermogravimetric analysis (TGA) experiments were carried out to follow the decomposition of $[Me_2Pt(COD)]$ and $[Me_2Pt(CNMe)_2]$ under various conditions, and the evolved gases were identified by FTIR (Table V).

$[Me_2Pt(COD)]$ melts at 100 °C, and the subsequent decomposition takes place in the temperature range 110–200 °C, leading to total elimination of the organic ligands. The weight loss by TGA was 42–44% compared to the theoretical value of 41.4%, and the DSC exotherm was simple (Figure 5). The evolved gases were identified as mostly methane and 1,5-cyclooctadiene by using FTIR. The decomposition of the complex under oxygen gave, in the later stages, some carbon dioxide presumably by oxidation of carbide or hydrocarbon in the platinum residue.

In contrast to the above, the decomposition of $[Me_2Pt(CNMe)_2]$ was complex, and at least three phases of decomposition could be noted. Experiments were carried out using nitrogen carrier gas and also mixtures of N_2/H_2 and N_2/O_2. Thus, with N_2 carrier gas, below 230 °C the evolved gas consisted of a mixture of ethane and methane with some MeNC. The second phase of decomposition occurred at 250–400 °C, giving rise to methane with some ethane and also MeNCO and CO_2. Above 400 °C the product contained mainly MeNCO and CO_2. A marked decrease in the decomposition temperature was noticed when the experiments were carried out in an oxygen atmosphere (Figure 6). Thus, in the temperature range 230–400 °C, a 30% weight loss was registered for decomposition in the presence of oxygen compared to 12% in absence of oxygen. The above results are qualitatively analyzed below.

(1) The first phase of decomposition (below 230 °C, under N_2) gives a weight loss corresponding to about one methyl group and a fraction of a MeNC ligand. At this stage, both methane and ethane are formed.

(2) In the next stage (250–380 °C under N_2) the major hydrocarbon product was methane with little ethane. In addition, the compounds MeNCO and CO_2 were observed. At this stage the total weight loss corresponded to the two

MePt groups and a fraction of an MeNC ligand or to one MePt group and one MeNC ligand.

(3) The later stages gave mostly MeNCO, CO_2, and H_2O as products. Under N_2, weight loss corresponding to formation of pure platinum metal was not complete until the temperature reached 700 °C. The weight loss clearly requires oxygen impurities in the N_2 carrier gas to give the observed products. This may involve slow oxidation of the polymeric material formed primarily from the MeNC ligands, as discussed earlier, or it may involve slow breakdown of Pt(MeNC) clusters or a combination of these reactions. Previous work has shown that the adsorption of MeNC on a platinum surface is irreversible and that only H_2 and HCN can be desorbed at high temperature (>400 K) under vacuum.[13,14]

(4) The decomposition under N_2/H_2 mixture was similar to that under N_2 (Table V) except that some $MeNH_2$ was detected, while the oxidation to give MeNCO, CO_2, and H_2O occurred much more easily under N_2/O_2 atmosphere, as expected. $MeNH_2$ is known to be decomposed on a platinum surface in the absence of hydrogen.[15]

The results of the solid-state thermolysis experiments using GC-MS or TGA-FTIR monitoring are in broad agreement, but there are also some differences that clearly result from the difference in experimental conditions.

On the Mechanism of Thermolysis. The thermal decomposition of dialkylplatinum(II) complexes in the solid state and in solution has been studied by several workers.[17,18] Several pathways may contribute to the thermolysis including homolytic fission of the metal–alkyl bond, reductive elimination by C–C bond formation, and α-, β- or γ-elimination reactions; the extent of each of these pathways is dependent on the nature of the alkyl group. It is interesting to compare the solid-, solution-, and gas-phase reactions. In the present study the solid-state decomposition behavior of the complexes can be described by

$$R(Me)PtL_2 \rightarrow R\text{–}H + R\text{–}R + CH_4 + L \text{ (or } L^*)$$

where R = methyl, allyl, vinyl; L = methyl isocyanide, xylyl isocyanide, 1,5-cyclooctadiene; and L* is derived from L either by polymerization (L = MeNC) or by combination with methylplatinum groups (L = XyNC giving XyN=CMe_2).[19] As discussed earlier, the thermolysis of 1 from the vapor probably occurs by preliminary ligand dissociation to give the coordinatively unsaturated complex [$PtMe_2$(MeNC)], which then decomposes further to give methane. Since the solid-state thermolysis of 1 gives much ethane in the early stages, it is not clear if this mechanism applies under these conditions. However, the preliminary ligand dissociation may well be common to all the gas-phase thermolyses and has previously been shown to occur in solution thermolyses of related compounds.[8,18] The absence of any significant product from coupling of the alkyl groups R and Me (in cases where R is not Me) rules out an intramolecular reductive elimination pathway, which has been demonstrated for some diarylplatinum and vinyl(alkynyl)platinum complexes.[17] A possible route to methane might involve α-elimination followed by reductive elimination: $PtMe_2 \rightarrow PtMe(CH_2)H \rightarrow MeH + Pt{=}CH_2$, but this is ruled out by the isotopic labeling experiments. A free-radical mechanism can account for the observed products when the thermolyses are carried out in the absence of hydrogen. Thus [PtMeRL] would give the radical R•, which could then combine to give R–R, whereas the more reactive radical Me• would abstract a hydrogen atom to give CH_4. However, it is likely that heterogeneous platinum-surface-catalyzed reactions are responsible for a large part of the reaction, and more experimental work is required to settle this issue.

Conclusions

The thermolysis of dialkylplatinum(II) complexes in the presence of hydrogen gives platinum films of high purity. These precursors therefore give a viable alternative to the use of the platinum(IV) precursors [$PtMe_3(C_5H_5)$] and [$PtMe_3(MeC_5H_4)$], which are also excellent.[7] One advantage of the platinum(II) complexes is the ease with which the thermal stability can be modified by choice of alkylplatinum groups. In addition, the photochemical stability can be modified easily by changing the supporting ligands. One disadvantage is that the platinum(II) precursors, even with low molecular weight ligands, have lower volatility than the platinum(IV) precursors. Both classes of precursor give excellent purity of the platinum films when CVD is carried out in the presence of hydrogen.

The thermolysis of the organoplatinum(II) complexes in the absence of hydrogen gives platinum films with considerable carbon impurities. To understand this problem, it is important to know the mechanism of the thermolysis. This paper has reported preliminary studies based primarily on product analyses and isotopic labeling. A more detailed study, including kinetic studies and studies of the surface binding of the precursors, will be published elsewhere.[20] The gas-phase thermolysis of *cis*-[$PtMe_2(MeNC)_2$] appears to involve preliminary reversible dissociation of an isocyanide ligand followed by formation of methane. A free-radical or surface-catalyzed mechanism for methane formation is possible, and it is proved that the extra hydrogen atom needed to convert a MePt group to methane is not derived from the second MePt group or from a MeNC ligand. In the presence of hydrogen, direct hydrogenation of a MePt group is indicated. At least some of the carbon impurity in the platinum film is shown to be derived from methylplatinum groups and is probably present as both carbide and CH_n residues.

Acknowledgment. We thank the Ontario Center for Materials Research and the NSERC (Canada) for financial support and Surface Science Western for assistance with the surface analytical work.

(13) Avery, N. R.; Matheson, T. W. *Surf. Sci.* **1984**, *143*, 110.
(14) Szilagyi, T. *Appl. Surf. Sci.* **1987**, *188*, 219.
(15) Hwang, S. Y.; Seebauer, E. G.; Schmidt, L. D. *Surf. Sci.* **1987**, *188*, 219
(16) Wilmshurst, J. K.; Bernstein, H. J. *Can. J. Chem.* **1957**, *35*, 226 and references therein. Although some bands of CH_4 and CH_3D occur at very similar frequencies, the rotational fine structure is distinctive and CH_3D has many extra bands (e.g., ν(CD)).
(17) (a) Stang, P. J.; Kowalski, M. H. *J. Am. Chem. Soc.* **1989**, *111*, 3356. (b) Braterman, P. S.; Cross, R. J.; Young, G. B. *J. Chem. Soc., Dalton Trans.* **1977**, 1892.
(18) (a) Schunn, R. A. *Inorg. Chem.* **1976**, *15*, 208. (b) Morrillo, A.; Turco, A. *J. Organomet. Chem.* **1983**, *258*, 383. (c) Morvillo, A.; Favero, G.; Turco, A. *J. Organomet. Chem.* **1983**, *243*, 111. (d) Komiya, S.; Morimoto, Y.; Yamamoto, A.; Yamamoto, T. *Organometallics* **1982**, *1*, 1528. (e) Whitesides, G. M. *Pure Appl. Chem.* **1981**, *53*, 287. (f) Miller, T. M.; Izumi, A. N.; Shih, Y.-S.; Whitesides, G. M. *J. Am. Chem. Soc.* **1988**, *110*, 3146.
(19) Alcock, N. W.; Brown, J. M.; MacLean, T. D. *J. Chem. Soc., Chem. Commun.* **1984**, 1689.
(20) Nixon, B.; Norton, P. R.; Ou, E. C.; Puddephatt, R. J.; Roy, S.; Young, P. A. *Chem. Mater.* **1991**, *3*, 222. This paper gives a preliminary account of kinetic studies.